Journal of Thermal Analysis and Calorimetry, Vol. 72 (2003) 241–251

THERMAL AND CONDUCTOMETRIC STUDIES OF $NdBr_3$ AND $NdBr_3$–LiBr BINARY SYSTEM

L. Rycerz[1*], *E. Ingier-Stocka*[1], *M. Cieślak–Golonka*[1] *and M. Gaune-Escard*[2]

[1]Institute of Inorganic Chemistry and Metallurgy of Rare Elements, University of Technology, Wybrzeze Wyspianskiego 27, 50-370 Wrocław, Poland
[2]Ecole Polytechnique, Méchanique & Energétique, Technopôle de Chateau-Gombert, 5 rue Enrico Fermi, 13453 Marseille Cedex 13, France

Abstract

The heat capacity of solid $NdBr_3$ was measured by Differential Scanning Calorimetry in the temperature range from 300 K up to the melting temperature. The heat capacity of liquid $NdBr_3$ was also determined. These results were least-squares fitted to a temperature polynome. The melting enthalpy of $NdBr_3$ was measured separately. DSC was used also to study phase equilibrium in the $NdBr_3$–LiBr system. The results obtained provided a basis for constructing the phase diagram of the system under investigation. It represents a typical example of simple eutectic system. The eutectic composition, $x(NdBr_3)$=0.278, was obtained from the Tamman construction. This eutectic mixture melts at 678 K. The electrical conductivity of $NdBr_3$–LiBr liquid mixtures and of pure components was measured down to temperatures below solidification. Reflectance spectra of the pure components and their solid mixtures (after homogenisation in the liquid state) with different composition were recorded in order to confirm the reliability of the constructed phase diagram.

Keywords: differential scanning calorimetry, electrical conductivity, fusion enthalpy, heat capacity, lithium bromide, neodymium bromide, phase diagram, thermodynamic functions

Introduction

We have previously measured and reported the enthalpies and entropies of fusion as well as heat capacity of almost all lanthanide(III) chlorides [1–4]. This work continues our general research program on lanthanide halides and their mixtures with alkali metal halides. It presents thermodynamic properties of neodymium(III) bromide, phase diagram of $NdBr_3$–LiBr binary system as well as electrical conductivity of pure $NdBr_3$ and it's mixtures with lithium bromide.

* Author for correspondence: E-mail: rycerz@ichn.ch.pwr.wroc.pl

1388–6150/2003/ $ 20.00
Akadémiai Kiadó, Budapest

Experimental

Neodymium(III) bromide was prepared from neodymium(III) oxide in a manner similar to that described previously [5]. No insoluble matter was found on dissolving it in water. The chemical analysis of the synthesised $NdBr_3$ was performed by titration methods for bromide (mercurimetric) and lanthanide (complexometric). These results are presented in Table 1.

Table 1 Chemical analysis of $NdBr_3$

Compounds	Mass%			
	$Br_{experimental}$	$Br_{theoretical}$	$Nd_{experimental}$	$Nd_{theoretical}$
$NdBr_3$	62.47	62.44	37.53	37.56

Lithium bromide was Merck Suprapur reagent (min. 99.9%). Before use, it was progressively heated up to fusion under gaseous HBr atmosphere. HBr in excess was then removed from the melt by argon bubbling.

The mixtures of $NdBr_3$ and LiBr (in appropriate proportions) were melted in vacuum-sealed quartz ampoules in an electric furnace. Melts were homogenised by shaking and solidified. These samples were ground in an agate mortar in a glove box. Homogenous mixtures of different composition prepared along the same procedure were used in phase diagram and electrical conductivity measurements.

All chemicals were handled in an argon glove box with a measured volume fraction of water of about $2 \cdot 10^{-6}$ and continuous gas purification by forced recirculation through external molecular sieves.

The enthalpy of fusion and the heat capacities were measured with a SETARAM DSC 121 Differential Scanning Calorimeter. The apparatus and the measurements procedure were described in details previously [2]. Quartz cells (about 6 mm diameter and 15 mm length) were filled with neodymium bromide in a glove-box, sealed under vacuum and then placed into the DSC 121 calorimeter.

Enthalpies of transition measurements were carried out with heating and cooling rates between 1 and 5 K min^{-1}.

The so-called 'step method' used for C_p measurements was already described [2, 6]. In this method, small heating steps are followed by isothermal delays, when thermal equilibrium of the sample is achieved. Two correlated experiments should be carried out to determine the heat capacity of the sample. The first one, with two empty cells with identical mass and the second with one of these cells loaded with the sample. The heat flux is recorded as a function of time and of temperature in both runs. The difference of heat flux in both runs is proportional to the amount of heat (Q_i) necessary to increase the temperature of the sample by a small temperature increment ΔT_i. Therefore, the heat capacity of the sample (C_p) is equal to:

$$C^0_{p,m} = (Q_i M_s)/(\Delta T_i m_s)$$

where m_s is the mass of the sample, M_s is the molar mass of the sample.

The same operating conditions (e.g. initial and final temperatures, temperature increment, isothermal delay and heating rate) are required for the two experimental runs. The original SETARAM program performs all necessary calculations. The apparatus was calibrated by the Joule effect. Additionally, some test measurements with NIST 720 α-Al_2O_3 Standard Reference material have been carried out separately prior to investigation [2]. According to this test, which gave C_p values consistent with standard data for Al_2O_3, the step method may be considered as suitable for C_p measurements.

Heat capacity measurements were performed by the 'step method'–each heating step of 5 K was followed by 400 s isothermal delay. The heating rate was 1.5 K min^{-1}. All experiments were started at 300 K and were performed up to 1100 K. The mass difference of the quartz cells in a particular experiment did not exceed 1 mg (mass of the cells: 400–500 mg). The mass of the samples was 200–500 mg.

Electrical conductivity measurements were carried out in capillary quartz cell described in details elsewhere [7]. The cell filled with the compound under investigation was placed into a furnace with a stainless steel block, used to achieve a uniform temperature distribution. The conductivity of the melt was measured by platinum electrodes with conductivity meter Tacussel CD 810. Experimental runs were conducted both upon heating and cooling regimes at rates ranging 1–2 K min^{-1}. The mean value of these two measurements was used in calculations. Temperature and conductivity data acquisition was made with a PC interfaced to the conductivity meter. The accuracy of electrical conductivity measurements was estimated at ±2%. Temperature was measured by means of a Pt/Pt-Rh thermocouple within the accuracy 1 K. Experimental cell was calibrated with a pure NaCl melt [8]. The resulting cell constant was 152 cm^{-1}. The same cell was used for all experiments and the cell constant checked from time to time in order to control any possible evolution. These measurements were carried out under static argon atmosphere.

Electronic reflectance spectra of powdered samples were measured with a Carry 500 Scan UV-vis-NIR Spectrophotometer (Varian) in the 8 000–50 000 cm^{-1} range. The scan rate was 3614 cm^{-1} min^{-1}, data interval 1 nm, slit width 2 nm.

Results and discussion

$NdBr_3$

As supercooling was observed in DSC cooling curves (about 25 K), temperature and fusion enthalpy of $NdBr_3$ were determined from heating DSC curves. $NdBr_3$ was found to melt at 956 K with the corresponding enthalpy and entropy of fusion $\Delta_{fus}H^0_m =$ 45.5 kJ mol^{-1} and $\Delta_{fus}S^0_m = 47.6$ J mol^{-1} K^{-1}, respectively. These results are in excellent agreement with data of Dworkin and Bredig obtained by means of a copper block drop calorimeter [9] (955 K, 45.6 kJ mol^{-1} and 47.7 J mol^{-1} K^{-1}, respectively).

Our experimental heat capacity values of $NdBr_3$ are plotted *vs.* temperature in Fig. 1, together with literature data [10] based on drop calorimetry measurements of Dworkin and Bredig [9]. An excellent agreement is observed for the solid phase. Our experimental heat capacity data for the liquid were averaged to the constant value

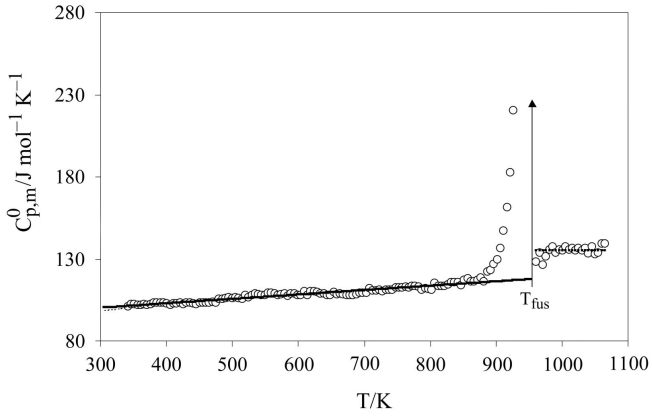

Fig. 1 Molar heat capacity of $NdBr_3$: ○ – experimental values; — – polynomial fitting of experimental values; ····· – literature data [10–11]

$C^0_{p,m}$=138.85 J K^{-1} mol^{-1}. This value is about 10 J K^{-1} mol^{-1} lower than heat capacity of liquid $NdBr_3$ given by Dworkin and Bredig [11].

The polynomial heat capacity dependence on temperature used by Barin *et al*. [10] for lanthanide halides:

$$C^0_{p,m} = a + b10^{-3}T + c10^5 T^{-2} \quad (1)$$

was also used by us to fit experimental data for solid $NdBr_3$. However, because of the strong C_p increase when approaching melting, only those data corresponding to a smooth heat capacity dependence on temperature were used.

The thermodynamic functions of $NdBr_3$ were calculated up to 1300 K using our experimental melting temperature and enthalpy together with heat capacity data. We determined the value $C^0_{p,m}$ (298.15 K) by extrapolation of our results to 298.15 K.

The standard entropy $S^0_m(NdBr_3,s,298.15\ K)$=196.65 J K^{-1} mol^{-1} was taken from literature [12].

The $C^0_{p,m}=f(T)$ equation was then used to calculate heat capacity $C^0_{p,m}(T)$ in J K^{-1} mol^{-1}, enthalpy increments $H^0_m(T)–H^0_m$, (298.15 K) in kJ mol^{-1}, entropy $S^0_m(T)$ and Gibbs energy functions $(G^0_m(T)–H^0_m(298.15))/T$ in J K^{-1} mol^{-1} both for solid as well as liquid $NdBr_3$. The corresponding equations are given below. The results for selected temperatures are presented in Table 2.

$NdBr_3$ solid, 298.15 K<T<956 K:

$$C^0_{p,m} = 92.59 + 26.50\cdot10^{-3}T - 0.176\cdot10^5 T^{-2}$$

$$H^0_m(T) - H^0_m(298.15) = 92.59\cdot10^{-3}T + 13.25\cdot10^{-6}T^2 + 0.176\cdot10^2 T^{-1} - 28.84$$

$$S^0_m(T) = 92.59\ln T + 26.50\cdot10^{-3}T + 0.088\cdot10^5 T^{-2} - 338.90$$

$$-(G^0_m(T) - H^0_m(298.15))/T = 92.59\ln T + 13.25\cdot10^{-3}T - 0.088\cdot10^5 T^{-2} + 288.43T^{-1} - 431.49$$

$NdBr_3$ liquid, 956 K<T<1300 K:

$$C^0_{p,m} = 138.85$$

$$H^0_m(T) - H^0_m(298.15) = 138.85 \cdot 10^{-3} T - 15.44$$

$$S^0_m(T) = 138.85 \ln T - 583.42$$

$$-(G^0_m(T) - H^0_m(298.15))/T = 138.85 \ln T + 15438 T^{-1} - 722.27$$

Having the thermodynamic functions for $NdBr_3$, one can calculate the thermodynamic functions of its formation as a function of temperature.

The formation of $NdBr_3$ from the elements can be described by the reaction:

$$Nd(s) + 1.5\ Br_2(l,g) = NdBr_3(s,l) \quad (2)$$

and the related thermodynamic functions of $NdBr_3$ formation depend on the thermodynamic functions of metallic Nd and bromine Br_2. The latter were calculated using literature data for $C^0_{p,m}$ and S^0_m(298.15 K) [13]. The enthalpy of $NdBr_3$ formation at 298.15 K, $\Delta_{form}H^0_m(NdBr_3,s,298.15\ K) = -864.0$ kJ mol^{-1}, also required in this calculation, was taken from Cordfunke and Konings recent work [14].

Four phase changes occur in this system described by reaction (2): boiling of bromine at 331 K (enthalpy of 29.56 kJ mol^{-1}), melting of $NdBr_3$ at 956 K, hcp→bcc solid-solid phase transition of Nd at 1128 K (with enthalpy of 3.0 kJ mol^{-1}) and melting of Nd at 1289 K (enthalpy of 7.1 kJ mol^{-1}) [13]. Accordingly, the formation enthalpy $\Delta_{form}H^0_m$ (kJ mol^{-1}) and Gibbs formation energy $\Delta_{form}G^0_m$ (kJ mol^{-1}) are described by the equations given below:

$NdBr_3$ solid, 298.15 K<T<331 K:

$$\Delta_{form}H^0_m = -35.66 \cdot 10^{-3} T - 0.21 \cdot 10^{-6} T^2 + 4.657 \cdot 10^2 T^{-1} - 854.9$$

$$\Delta_{form}G^0_m = -133.49 \cdot 10^{-3} T + 0.21 \cdot 10^{-6} T^2 + 2.328 \cdot 10^2 T^{-1} + 35.659 \cdot 10^{-3} T \ln T - 854.9$$

$NdBr_3$ solid, 331 K<T<956 K:

$$\Delta_{form}H^0_m = 21.89 \cdot 10^{-3} T - 0.555 \cdot 10^{-6} T^2 + 2.707 \cdot 10^2 T^{-1} - 902.9$$

$$\Delta_{form}G^0_m = 346.19 \cdot 10^{-3} T + 0.555 \cdot 10^{-6} T^2 + 1.353 \cdot 10^2 T^{-1} - 21.896 \cdot 10^{-3} T \ln T - 902.9$$

$NdBr_3$ liquid, 956 K<T<1128 K:

$$\Delta_{form}H^0_m = 68.15 \cdot 10^{-3} T - 13.809 \cdot 10^{-6} T^2 + 2.531 \cdot 10^2 T^{-1} - 889.5$$

$$\Delta_{form}G^0_m = 636.96 \cdot 10^{-3} T + 13.805 \cdot 10^{-6} T^2 + 1.265 \cdot 10^2 T^{-1} - 68.154 \cdot 10^{-3} T \ln T - 889.5$$

$NdBr_3$ liquid, 1128 K<T<1289 K:

$$\Delta_{form}H^0_m = 38.23 \cdot 10^{-3} T - 0.345 \cdot 10^{-6} T^2 - 1.95 \cdot 10^2 T^{-1} - 875.4$$

Table 2 Thermodynamic functions of $NdBr_3$ at selected temperatures from 298.15 to 1300 K

T/K	$C^0_{p,m}(T)$ / J K^{-1} mol^{-1}	$S^0_m(T)$ / J K^{-1} mol^{-1}	$(-(G^0_m(T)-H^0_m(298.15)$/ J K^{-1}mol^{-1}	$H^0_m(T)-H^0_m(298.15)$/ kJ mol^{-1}	$\Delta_{form}H^0_m(T)$ / kJ mol^{-1}	$\Delta_{form}G^0_m(T)$ / kJ mol^{-1}
298.15	100.29	196.65	196.65	0.00	–864.0	–833.4
300	100.35	197.27	196.65	0.19	–864.1	–833.2
331	101.20	207.18	197.18	3.31	–865.3	–829.9
331	101.20	207.18	197.18	3.31	–894.9	–829.9
400	103.08	226.51	200.62	10.36	–893.5	–816.5
500	105.77	249.80	208.20	20.80	–891.5	–797.5
600	108.44	269.32	216.81	31.51	–889.5	–778.8
700	111.11	286.24	225.54	42.49	–887.5	–760.5
800	113.76	301.25	234.09	53.73	–885.4	–742.5
900	116.42	314.80	242.31	65.24	–883.3	–724.8
956	117.91	321.88	246.77	71.80	–882.2	–715.0
956	138.85	369.48	246.77	117.30	–836.7	–715.0
1000	138.85	375.72	252.31	123.41	–834.9	–709.4
1100	138.85	388.96	264.14	137.30	–831.0	–697.1
1128	138.85	392.45	267.28	141.18	–830.0	–693.7
1128	138.85	392.45	267.28	141.18	–832.9	–693.7
1200	138.85	401.04	275.05	151.18	–830.2	–684.9
1289	138.85	410.97	284.09	163.54	–826.9	–674.2
1289	138.85	410.97	284.09	163.54	–834.0	–674.2
1300	138.85	412.15	285.17	165.07	–833.7	–672.8

$$\Delta_{\text{form}} G_{\text{m}}^{0} = 429.57 \cdot 10^{-3} T + 0.345 \cdot 10^{-6} T^{2} - 0.975 \cdot 10^{2} T^{-1} - 38.234 \cdot 10^{-3} T \ln T - 875.4$$

$NdBr_3$ liquid, 1289 K<T<1300 K:

$$\Delta_{\text{form}} H_{\text{m}}^{0} = 34.05 \cdot 10^{-3} T - 0.345 \cdot 10^{-6} T^{2} - 1.95 \cdot 10^{2} T^{-1} - 877.2$$

$$\Delta_{\text{form}} G_{\text{m}}^{0} = 400.93 \cdot 10^{-3} T + 0.345 \cdot 10^{-6} T^{2} - 0.975 \cdot 10^{2} T^{-1} - 34.05 \cdot 10^{-3} T \ln T - 877.2$$

The results obtained for selected temperatures are presented in Table 2.

$NdBr_3$–LiBr system

The phase diagrams of $NdBr_3$ with alkali metal bromides (M=Na, K, Rb, Cs) were determined by Vogel [15] as well as by Blachnik and Jaeger-Kasper [16]. However the $NdBr_3$–LiBr phase diagram was established for the first time in the course of the present work. The DSC investigations performed on samples with 19 compositions yielded both the temperature and the fusion enthalpy of the concerned mixtures. The values of enthalpies of thermal effects obtained from heating and cooling curves were almost the same, the difference between them being no more than 2%. However, supercooling was observed on cooling curves. Due to this supercooling effect, all values of temperature and enthalpy given in this work were determined from the heating curves.

The phase diagram of the system under investigation was found to be simple eutectic type. In the whole range of compositions, only two peaks ascribed to the eutectic and the liquidus effects were found in every DSC curve. The eutectic contribution to the enthalpy of fusion was determined and plotted against the composition in Fig. 2. This so-called Tamman construction makes it possible to evaluate accurately the eutectic composition from the intercept of the two linear parts in Fig. 2, described by the equations $\Delta_{\text{fus}} H_{\text{m}}^{0} = 74.01 x(\text{NdBr}_3)$ and $\Delta_{\text{fus}} H_{\text{m}}^{0} = 28.51 - 28.51 x(\text{NdBr}_3)$ in kJ mol^{-1}, respectively. In the above equations $x(\text{NdBr}_3)$ denotes molar fraction of neodymium tribromide. We obtained $x(\text{NdBr}_3)$=0.278 for the eutectic composition while the eutectic temperature determined from all the appropriate DSC curves is T_{eut}=678 K. The enthalpy of fusion at

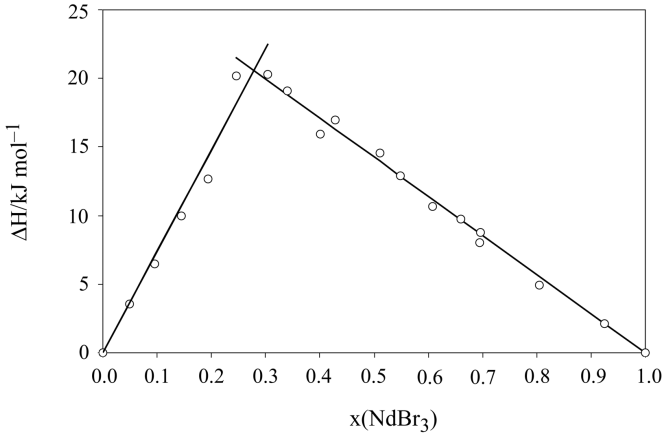

Fig. 2 Tamman construction for eutectic in $NdBr_3$–LiBr system

the eutectic composition is $\Delta_{fus}H^0_m$=20.6 kJ mol^{-1}. In this Tamman construction it was assumed that there was no solubility in the solid state. Thus straight lines intercept the composition axis at $x(NdBr_3)$=0 and $x(NdBr_3)$=1.

The complete phase diagram of $TbBr_3$–NaBr binary system is presented in Fig. 3.

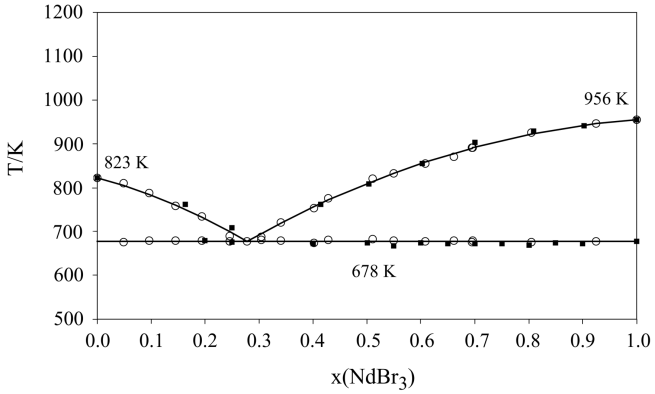

Fig. 3 Phase diagram of $NdBr_3$–LiBr system: ○ – DSC method; ■ – electric conductivity method

The electronic spectra for several mixtures of $NdBr_3$ and LiBr were registered in order to confirm the reliability of the constructed phase diagram. The reflectance spectra of pure $NdBr_3$ and pure LiBr salts, the mixture of $NdBr_3$ (20 mol%) and LiBr (80 mol%) and finally, the mixture of 70 mol% $NdBr_3$ and 30 mol% LiBr (the mixtures were melted, cooled and powdered before measuring the spectra) are presented in Figs 4a, b and c, respectively. The comparison of the spectra shows that the main difference between them is the intensity of the bands which decrease in the sequence: a>c>b, i.e. it is dependent exclusively upon the amount of $NdBr_3$, just as expected for two component mixtures. The spectra are very well resolved both in their f-f and CT($Br\rightarrow Nd^{3+}$) absorption regions (LiBr has its CT transitions in the higher energy region). Moreover, the spectrum of $NdBr_3$ within 25000–33000 cm^{-1} uncovers the higher energy f-f transitions usually overlapped in the complexes with the CT bands of the organic ligands. From the lowest CT$\pi Br\rightarrow Nd^{3+}$ transition at ca 37000 cm^{-1} the optical electronegativity χ of the Nd^{3+} accepted orbital can be calculated from the formula: ν_{CT}=30000 [$\chi_{opt}(Br^-)$–$\chi_{opt}(M)$] cm^{-1} (LMCT) [17]. As χ value for the bromide anion π orbitals is 2.8 the optical electronegativity for Nd^{3+} is 1.56 which lies in the range characteristic for trivalent lanthanide ions. The presence of only the bands characteristic for $NdBr_3$ over the entire composition range of mixtures confirms that the system is a simple eutectic type.

The electrical conductance of the liquid phase of pure $NdBr_3$ was measured. These data were fitted by polynomial Eq. (3):

$$\kappa = -1.083+1.377\cdot10^{-3}T+1.896\cdot10^{-7}T^2 \quad (3)$$

The determined specific conductivity data presented in Fig. 5 are in good agreement with Dworkin *et al*. [18]. However they are lower than presented by Vogel [19].

Preliminary investigations of electrical conductivity of the liquid phase of $NdBr_3$–LiBr mixtures (over the entire composition range) were also performed. The spe-

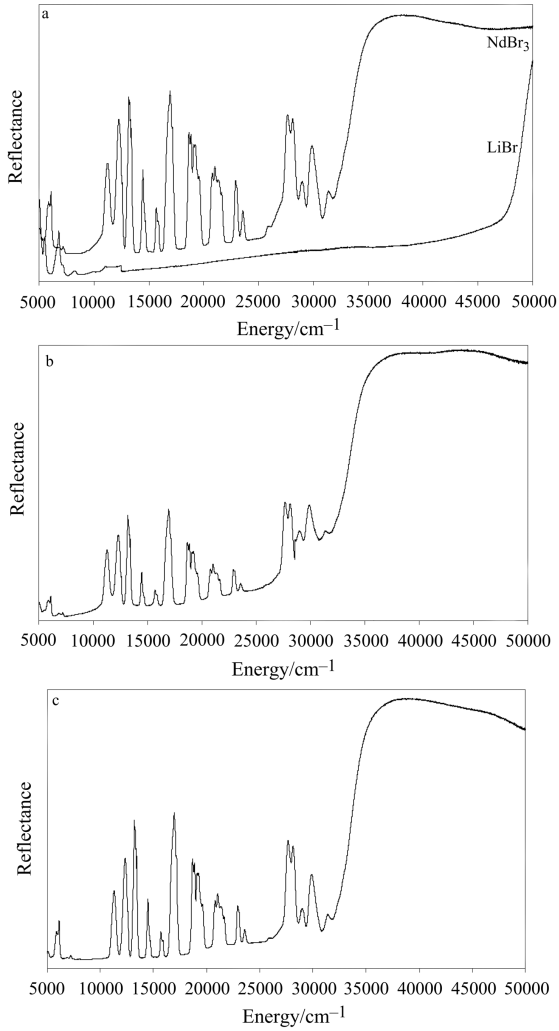

Fig. 4 Reflectance spectra of powdered samples: a – pure $NdBr_3$ and pure LiBr; b – the mixture of 20 mol% $NdBr_3$ and 80 mol% LiBr after melting; c – the mixture of 70 mol% $NdBr_3$ and 30 mol% LiBr after melting

cific conductivity dependence on composition at temperature 1000 K is shown in Fig. 6. Generally, the κ value decreases with increasing of $NdBr_3$ concentration. These studies are continued and their detailed discussion will be done in future together with liquid phase conductivity data of the others $NdBr_3$–MBr systems (where *M*=Na, K, Rb, Cs). The solid phase conductivity was also examined at some compositions for the purpose of correlating the characteristic temperatures determined by DSC to those observed with this new technique. As it can be seen (Fig. 3) a quite good compatibility was obtained.

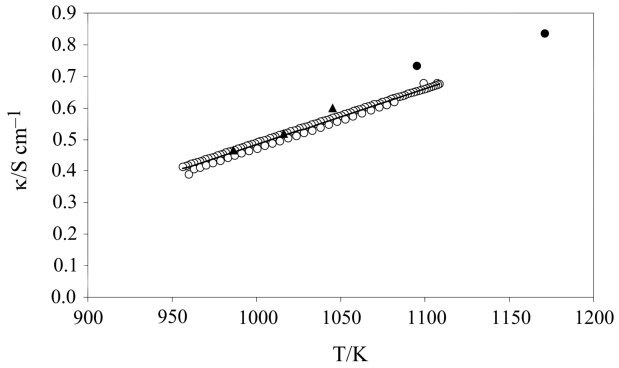

Fig. 5 Specific conductivity of pure $NdBr_3$ (liquid phase): ○ – experimental values; ▲ – literature data [18]; ● – literature data [19]

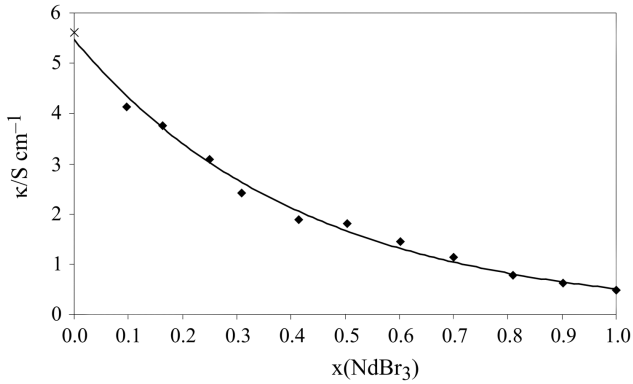

Fig. 6 Specific conductivity of $NdBr_3$–LiBr mixtures at 1000 K: ◆ – experimental values; × – literature data [20–21]

The fusion temperatures determined were as follows: T_{fus}($NdBr_3$)=956 K (DSC) and 956 K (cond.); T_{fus}(~25 mol% $NdBr_3$)=677 K (DSC) and 680 K (cond.); T_{fus}(~61 mol% $NdBr_3$)=678 K (DSC) and 682 K (cond.). The same similarity was with the liquidus temperatures, e.g. T_{liq}(~60 mol% $NdBr_3$)=855 K (DSC) and 855 K (cond.); T_{liq}(~81 mol% $NdBr_3$)=926 K (DSC) and 929 K (cond.).

Conclusions

The values of $C^0_{p,m}$ (solid and liquid $NdBr_3$), T_{fus}, $\Delta_{fus}H^0_m$, $\Delta_{fus}S^0_m$ were determined. Also, the thermodynamic functions of $NdBr_3$ were calculated up to 1300 K.

The investigations of the $NdBr_3$–LiBr system carried out by several methods (DSC, spectroscopy, electrical conductivity) made it possible to construct a phase diagram of the system. The conductometry and spectroscopy as the subsidiary methods proved to be proper to confirm the results obtained by DSC method. It was revealed that the $NdBr_3$–LiBr system was a simple eutectic type. The eutectic composition,

$x(NdBr_3)$=0.2781, was determined by the Tamman method. This eutectic mixture melts at 678 K with the corresponding enthalpy of about 20.58 kJ mol^{-1}. The determined specific electrical conductivity of the liquid $NdBr_3$ fitted by the quadratic function of temperature agrees with the literature data [18] very well.

* * *

Part of us (LR, EI-S and MG-C) acknowledges support from the Polish Committee for Sciencific Research under the Grant 3 T09A 091 18. LR also wishes to thank the Ecole Polytechnique de Marseille for hospitality and support during this work.

References

1 M. Gaune-Escard, L. Rycerz, W. Szczepaniak and A. Bogacz, J. Alloys Comp., 204 (1994) 193.
2 M. Gaune-Escard, A. Bogacz, L. Rycerz and W. Szczepaniak, J. Alloys Comp., 235 (1996) 176.
3 L. Rycerz and M. Gaune-Escard, Z. Naturforsch., 57 a (2002) 79.
4 L. Rycerz and M. Gaune-Escard, Z. Naturforsch., 57 a (2002) 215.
5 L. Rycerz and M. Gaune-Escard, J. Therm. Anal. Cal., 56 (1999) 355.
6 M. Gaune-Escard and L. Rycerz, Z. Naturforsch., 54 a (1999) 229.
7 Y. Fouque, M. Gaune-Escard, W. Szczepaniak and A. Bogacz, J. Chim. Phys., 75 (1978) 360.
8 G. J. Janz, Materials Science Forum, 73–75 (1991) 707.
9 A. S. Dworkin and M. A. Bredig, High Temp. Sci., 31 (1971) 81.
10 I. Barin, O. Knacke and O. Kubaschewski, Thermochemical Properties of Inorganic Substances, Supplement, Springer - Verlag Berlin, Heidelberg, New York 1977.
11 A. S. Dworkin and M. A. Bredig, J. Phys. Chem., 67 (1963) 2499.
12 C. E. Wick and F. E. Block, Thermodynamic Properties of 65 Elements – Their Oxides, Halides, Carbides and Nitrides, Bureau of Mines, Bull. 605, US Gov. Printing Office, Washington 1963.
13 O. Kubaschewski, C. B. Alcoock and P. J. Spencer, Materials Thermochemistry, 6th Edition, Pergamon Press Ltd, 1993.
14 E. H. P. Cordfunke and R. J. M. Konings, Thermochim. Acta, 375 (2001) 17.
15 G. Vogel, Z. Anorg. Allg. Chem., 388 (1972) 43.
16 R. Blachnik and A. Jaeger-Kasper, Z. Anorg. Allg. Chem., 461 (1980) 74.
17 A. B. P. Lever, Inorganic Electronic Spectroscopy, 2nd Ed. Elsevier, Amsterdam, Oxford, New York, Tokyo 1984.
18 A. S. Dworkin, H. R. Bronstein and M. A. Bredig, J. Phys. Chem., 67 (1963) 2715.
19 G. Vogel, Diss. Clausthal T. K. 1970, p. 68.
20 G. J. Janz, NIST Standard Reference Database 27, Version 2.0 (1992).
21 I. S. Yaffe, E. R. Van Artsdalen ORNL – 2159 (1956) 77.